A newly characterized dense granule protein (GRA76) is important for the growth and virulence of *Toxoplasma gondii*

Xiao-Nan Zheng [a b,] Li-Xiu Sun [a c,] Hany M. Elsheikha [d,] Ting-Ting Li [a e,] Jin Gao [a b,] Xiao-Jing Wu [a b,] Zhi-Wei Zhang [a,] Meng Wang [a e,] Bao-Quan Fu [a e,] Xing-Quan Zhu [b,] Jin-Lei Wang [a e]

[a] State Key Laboratory for Animal Disease Control and Prevention, Lanzhou Veterinary Research Institute, Chinese Academy of Agricultural Sciences, Lanzhou, Gansu Province 730046, People′s Republic of China

[b] Laboratory of Parasitic Diseases, College of Veterinary Medicine, Shanxi Agricultural University, Taigu, Shanxi Province 030801, People′s Republic of China

[c] Research Center for Parasites & Vectors, College of Veterinary Medicine, Hunan Agricultural University, Changsha, Hunan Province 410128, People′s Republic of China

[d] Faculty of Medicine and Health Sciences, School of Veterinary Medicine and Science, University of Nottingham, Sutton Bonington Campus, Loughborough, LE12 5RD, UK

[e] Institute of Urban Agriculture, Chinese Academy of Agricultural Sciences, Chengdu, Sichuan Province 610213, People′s Republic of China

Abstract

Pathogenicity of the zoonotic pathogen *Toxoplasma gondii* largely depends on the secretion of effector proteins into the extracellular milieu and host cell cytosol, including the dense granule proteins (GRAs). The protein-encoding gene TGME49_299780 was previously identified as a contributor to parasite fitness. However, its involvement in parasite growth, virulence and infectivity in vitro and in vivo remains unknown. Here, we comprehensively examined the role of this new protein, termed GRA76, in parasite pathogenicity. Subcellular localization revealed high expression of GRA76 in tachyzoites inside the parasitophorous vacuole (PV). However, its expression was significantly decreased in bradyzoites. A CRISPR-Cas9 approach was used to knock out the *gra76* gene in the *T. gondii* type I RH strain and type II Pru strain. The in vitro plaque assays and intracellular replication showed the involvement of GRA76 in replication of RH and Pru strains. Deletion of the *gra76* gene significantly decreased parasite virulence, and reduced the brain cyst burden in mice. Using RNA sequencing, we detected a significant increase in the expression of bradyzoite-associated genes such as BAG1 and LDH2 in the PruΔ*gra76* strain compared with the wild-type Pru strain. Using an in vitro bradyzoite differentiation assay, we showed that loss of GRA76 significantly increased the propensity for parasites to form bradyzoites. Immunization with PruΔ*gra76* conferred partial protection against acute and chronic infection in mice. These findings show the important role of GRA76 in the pathogenesis of *T. gondii* and highlight the potential of PruΔ*gra76* as a candidate for a live-attenuated vaccine.

Keywords

Dense granule proteins
GRA76
Replication
Virulence
Bradyzoite differentiation
Toxoplasma gondii
Vaccine

1. Introduction

Toxoplasma gondii, the causative agent of toxoplasmosis, chronically infects one-third of the world's human population (Robert-Gangneux and Darde, 2012; Wang ZD, 2017; Elsheikha et al., 2021). *Toxoplasma gondii* encompasses three main lifecycle stages. Tachyzoites, the rapidly replicating form of *T. gondii*, are essential for acute infection (Robert-Gangneux and Darde, 2012, Elsheikha et al., 2021). Bradyzoites enclosed within tissue cysts are responsible for chronic infection (Elsheikha et al., 2021). Sporozoites-containing oocysts, the product of parasite sexual reproduction in the feline gut, are

shed in cat faeces and infect many intermediate hosts (Robert-Gangneux and Darde, 2012; Wang ZD, 2017; Elsheikha et al., 2021). The ingestion of sporulated oocysts in water or food contaminated with feline feces, or ingestion of tissue cysts in raw infected meat, results in horizontal transmission of infection to humans (Robert-Gangneux and Darde, 2012). When a pregnant woman is infected, tachyzoites can colonize the placenta and infect the fetus, leading to a detrimental health impact on the offspring (Robert-Gangneux and Darde, 2012). Primary *T. gondii* infection in immunocompetent individuals is often asymptomatic. However, switching of bradyzoites within the cysts back to tachyzoites can lead to life-threatening brain pathologies in immunocompromised individuals (Luft and Remington, 1992; Wang ZD, 2017; Elsheikha et al., 2021). Because none of the current therapies can eliminate parasite cysts, there is a clear need for better understanding of the mechanisms of *T. gondii* pathogenesis and identification of the virulence factors controlling tachyzoite transformation into bradyzoite-containing cysts.

The ability of *T. gondii* to infect a broad range of host cell types is mediated by sequential secretion of effector proteins including microneme proteins (MICs), rhoptry neck proteins (RONs), rhoptry body proteins (ROPs) and dense granule proteins (GRAs) (Bradley et al., 2005, Clough and Frickel, 2017, Bullen et al., 2019, Wang et al., 2020d). Once inside the host cell, the parasite replicates inside a parasitophorous vacuole (PV) surrounded by a parasitophorous vacuole membrane (PVM) (Clough and Frickel, 2017, Wang et al., 2020d). After GRAs are released from the dense granules and secreted into the PV lumen, some of GRAs are associated with the PVM and intravacuolar network (IVN), which connects the parasites and the PVM inside the PV (Clough and Frickel, 2017, Wang et al., 2020d, Griffith et al., 2022). In addition to these GRAs in the PV, IVN or PVM, some GRAs such as GRA16, GRA18 and GRA24 are exported into the host cells and hijack cellular immune functions (Clough and Frickel, 2017, Hakimi et al., 2017).

GRAs promote *T. gondii* survival and replication by modifying the functions of the PV, IVN, PVM and host cell environment. For example, GRA17 and GRA23 facilitate diffusion of small molecules and nutrients across the PVM (Gold et al., 2015). GRA14 and GRA64 are indispensable for the internalization of host cytosolic proteins by interacting with components of the host endosomal sorting complex required for transport (ESCRT) (Rivera-Cuevas et al., 2021, Mayoral et al., 2022). In addition to their roles in vesicle trafficking and nutrient acquisition, some GRAs are involved in trafficking and export of secreted proteins into the host cell or the PVM. The Myc regulation 1 (MYR) complex on PVM, encompassing MYR1, MYR2 and MYR3, interacts with GRA44, GRA45 and TgPPM3C, and forms a putative PVM-localized translocon, which is necessary for trafficking of effectors such as GRA16, GRA18, *T. gondii* inhibitor of STAT transcription (TgIST) and *Toxoplasma* E2F4-asociated EIH2-inducing gene regulator (TEEGR) (Blakely et al., 2020, Cygan et al., 2020, Wang et al., 2020d). The effectors GRA16, GRA24, TEEGR and TgIST translocate to the host cell nucleus, and manipulate host signal pathways and gene expression to counter the host immune system (Clough and Frickel, 2017, Wang et al., 2020d). Several secreted GRAs, which localize in host cells or PVMs, can subvert

the host immune response. GRA7 and GRA60, virulence factors of *T. gondii*, enable the parasites to evade the host innate immune mechanism by targeting the immunity regulated GTPases (Alaganan et al., 2014, Nyonda et al., 2021).

While functions of known GRAs have been characterized in the tachyzoite stage, some of them are also important in bradyzoites. In the bradyzoite stage, the IVN and PVM localized GRAs are located in the cyst wall and deletion of these *gra*s, such as GRA2, GRA5, GRA7, GRA8 and GRA14, affect accumulation of cyst wall proteins at the cyst periphery (Guevara et al., 2019, Guevara et al., 2020). In addition, some bradyzoite-specific GRA proteins are involved in cyst formation and persistence, including CST1 (Tomita et al., 2013) and GRA55 (Nadipuram et al., 2020). CST2/GRA50 and GRA55 are important virulence factors, affecting the establishment and maintenance of cysts in chronic infection (Tu et al., 2019, Nadipuram et al., 2020). Although significant progress has been made to uncover the mechanism of cyst formation, only a few cyst wall proteins have been identified and their involvement in parasite differentiation and cyst formation remains unknown.

In recent years, multiple novel *T. gondii* GRAs have been reported (Barylyuk et al., 2020), including a novel gene *TGME49_299780* which was predicted as a putative GRA using hyperplexed Localisation of Organelle Proteins by Isotopic Tagging (hyperLOPIT) (Barylyuk et al., 2020) and identified as a contributing factor to *T. gondii* fitness (Young et al., 2019, Butterworth et al., 2022). However, the function of this putative GRA (termed GRA76) remains unknown. In this study, we characterized the role of GRA76 in pathogenicity of *T. gondii* infection using CRISPR-Cas9 technology, immunofluorescence assay (IFA), plaque assay, intracellular replication assay, invasion assay, and egress assay. We also analyzed the effect of deletion of g*ra76* on the expression of bradyzoites-associated genes in PruΔ*gra76* using RNA sequencing (RNA-Seq). Our findings suggest that the newly characterized GRA76 plays a role in parasite growth, virulence, and bradyzoite differentiation.

2. Materials and methods

2.1. Animals

Kunming female mice (8 weeks of age) were obtained from the Center of Laboratory Animals, Lanzhou Veterinary Research Institute, Chinese Academy of Agricultural Science, China. Mice were housed in groups of six in polycarbonate microisolator cages with autoclaved bedding and enrichment material. Sterilized water and food were provided ad libitum. All mice were allowed to acclimate for 7 days prior to use. Mice were monitored twice daily, and the cage padding were changed every 2 days. All animal experiments were reviewed and approved by the Animal Research Ethics Committee of Lanzhou Veterinary Research Institute, Chinese Academy of Agricultural Sciences (Approval no. 2021-008). Every effort was made to alleviate the suffering of the animals during the study.

2.2. Maintenance of the parasite culture

The parental parasite strains RHΔ*ku80* and PruΔ*ku80* (noted as RH and Pru) and modified strains were grown in confluent monolayers of human foreskin fibroblasts (HFFs, ATCC SCRC-1041™) maintained in DMEM (Gibco, China) supplemented with 2% fetal bovine serum (FBS, Gibco, New Zealand), 10 mM HEPES (pH 7.2, Solarbio, China), 100 U/mL of penicillin (Solarbio, China) and 100 μg/mL of streptomycin (Solarbio, China) as described previously (Wang et al., 2020a). To isolate tachyzoites, heavily infected HFF monolayers were scraped from the tissue culture flask and passed through a 27-gauge needle (BD Medical, USA) to release the parasites from the host cells (Zheng et al., 2023).

2.3. Endogenous tagging

To construct a specific tagging CRISPR plasmid, the guide RNA targeting the locus near the stop codon of the *gra76* gene was cloned into the pSAG1::CAS9-U6-SgUPRT plasmid to replace the original guide RNA targeting the uracil phosphoribosyl transferase (UPRT) locus (Zheng et al., 2023). The pLIC-6HA-DHFR plasmid was used as a template to amplify the homologous fragments including the dihydrofolate reductase (DHFR) locus and the 6×hemagglutinin (HA) locus using specific primers with overhangs to the 5′ or 3′ locus of *gra76* gene (Zheng et al., 2023). The validated CRISPR tagged plasmids were collected by Endo-free Plasmid DNA Mini Kit (Omega, Switzerland), and the insertional cassettes were extracted by Gel Extraction Kit (Omega, Switzerland). The specific tagged CRISPR plasmid (~35 μg), together with the homologous fragments (~20 μg), were transfected into the tachyzoites of RHΔ*ku80* or PruΔ*ku80* strains via electroporation (BTX, USA) (Zheng et al., 2023). After selection using 3 μM pyrimethamine (Sigma, Germany), the independent clones of the tagged transfected parasites (RH::GRA76-HA or Pru::GRA76-HA) were obtained using 96-well tissue culture plates (Thermo Fisher Scientific, USA) and the modified limiting dilution method, and were confirmed by PCRs, sequencing, IFA, and western blots. All primers used are listed in Supplementary Table S1.

2.4. Gene disruption

CRISPR-Cas9 mediated homologous replacements were used to generate the *gra76*knockout strains as previously described (Wang et al., 2022, Zheng et al., 2023). Briefly, a CRISPR plasmid and a homologous DHFR selective plasmid were constructed. The gene knockout CRISPR plasmid (pSAG1::CAS9-U6-SgGRA76) designed against the middle exon locus of GRA76 was generated using the template pSAG1:CAS9-U6-SgUPRT plasmid. The homologous drug-selective plasmid was constructed by fusing the pUC19 fragment, the DHFR fragment, the 5′ and 3′ homologous arms of GRA76 by a CloneExpress II one-step Cloning Kit (Vazyme, China). After sequencing, the drug-selective plasmid was used as a template plasmid to amplify the homologous drug-selective cassette.

To delete the *gra76*, the sequencing validated pSAG1:CAS9-U6-SgGRA76 plasmids and the homologous drug-selective fragments were co-transfected into the RHΔ*ku80* or PruΔ*ku80* tachyzoites. After selection with pyrimethamine, single clones of RHΔ*ku80*Δ*gra76* or PruΔ*ku80*Δ*gra76*, referred to RHΔ*gra76* and PruΔ*gra76*, were selected from the transfected populations in 96-well plates using modified limiting dilution, and confirmed by diagnosed PCR. The primers used are listed in Supplementary Table S1.

2.5. Complementation of the knockout strains

To complement the knockout strain, a wild-type copy of GRA76 with a C-terminal 3×HA epitope tag which was driven by its own promoter or the *Toxoplasma* tubulin promoter, together with a chloramphenicol acetyl transferase (CAT) cassette encoding chloramphenicol resistance, were used to replace the hypoxanthine-xanthine-guanine phosphoribosyl transferase (HXGPRT) or UPRT locus of RHΔ*gra76* or PruΔ*gra76* using CRISPR-Cas9 (Wang et al., 2020a). To construct the pTub-GRA76-3HA-CAT plasmid, the *T. gondii* cDNA was amplified using the parasite total RNA as a template (Wang et al., 2020a). The coding sequence of GRA76 was amplified from the cDNA using specific primers with overhangs to the pTub-3HA-CAT backbone. The amplified fragments were then fused with the pTub-3HA-CAT vector backbone to generate the pTub-GRA76-3HA-CAT plasmid. A GRA76 promoter fragment amplified from *T. gondii* DNA was fused to the GRA76-3HA-CAT vector backbone which was amplified from the validated pTub-GRA76-3HA-CAT plasmid. These validated complemented plasmids were then used as a template to amplify the insertional cassette with primers that included homology segments to the UPRT or HXGPRT locus of *T. gondii*. The CRISPR vector (pSAG1:CAS9-U6-SgUPRT) targeting the UPRT locus or the vector (pSAG1:CAS9-U6-SgHXGPRT) targeting the HXGPRT locus was co-transfected with the PCR amplicon of pTub-GRA76-3HA-CAT or pGRA76-GRA76-3HA-CAT into tachyzoites of RHΔ*gra76* or PruΔ*gra76*. After several cycles of selection with chloramphenicol (Sigma, Germany), the independent clones (RHΔ*gra76*C, PruΔ*gra76*C or PruΔ*gra76*C_{Tub}) obtained by modified limiting dilution were confirmed by PCR, IFA, and western blots. Primers used to construct the complemented strains are listed in Supplementary Table S1.

2.6. Cyst differentiation in vitro

Bradyzoite-containing cysts were differentiated from tachyzoites in vitro as previously described (Wang et al., 2022, Zheng et al., 2023). Briefly, HFFs cultured on coverslips placed at the bottom of the wells of 12-well culture plates (Thermo Fisher Scientific, USA) were infected with tachyzoites for 4 h. The culture medium was then replaced with differentiated alkaline medium (pH 8.2). Cysts were differentiated at 37 °C in ambient air for 2 days. The IFA was then used to visualize the induced cysts. To quantify cyst differentiation, at least 100 vacuoles of each sample were randomly selected to

calculate the percentages of FITC-*Dolichos Biflorus* agglutinin (FITC-DBA, Vectorlabs, USA) positive cysts in three independent experiments.

2.7. Western blot analysis

Toxoplasma gondii parasites were harvested from cultured cells to detect protein expression by using SDS-PAGE and western blots. To detect the HA-tagged protein, freshly egressed parasites collected from normal or differentiation culture conditions were processed and analyzed using SDS-PAGE and western blots. This procedure was repeated three times independently, following previously described methods (Zheng et al., 2023).

2.8. IFA

The infected HFF monolayers were fixed with 4% paraformaldehyde (PFA, Sigma, Germany) for 20 min, permeabilized with 0.2% Triton X-100 (Sigma, Germany) for 15 min at room temperature (R.T.) (Wang et al., 2022). Samples were blocked with 3% BSA (Amresco, USA) in PBS and incubated with primary antibodies for 2 h prior to incubation with secondary antibodies for 1 h at 37 °C. Each procedure was followed by five washes with PBS. After the final wash, samples were imaged using a Leica confocal microscope system (TCS SP8, Leica, Germany). Polyclonal rabbit anti-GRA12 and polyclonal rabbit anti-GRA5 were available in our laboratory (Wang et al., 2020a). To assess subcellular localization of GRA76 (Wang et al., 2020a, Krishnamurthy et al., 2023), HA-tagged protein was detected by mouse anti-HA (1:500, Thermo Fisher Scientific, USA) and secondary goat anti-mouse IgG (H+L) antibodies conjugated with Alexa Fluor 594 (1:500, Thermo Fisher Scientific, USA). As GRA protein markers, GRA5 and GRA12 were detected with primary antibodies, rabbit anti-GRA5 (1:500) and rabbit anti-GRA12 (1:500), and secondary donkey anti-rabbit IgG (H+L) antibodies conjugated to Alexa Fluor 488 (1:500, Thermo Fisher Scientific, USA) in tachyzoites or goat anti-rabbit IgG (H+L) antibodies conjugated to Alexa Fluor 647 (1:500, Thermo Fisher Scientific, USA) in bradyzoites. FITC-DBA (1:500) that specifically recognizes N-acetylgalactosamine on the bradyzoite cyst wall was used to stain cysts (Guevara et al., 2020, Guevara et al., 2021). DNA was detected by DAPI (1:500, Thermo Fisher Scientific, USA) which was incubated after secondary antibodies. To check GRA16 and GRA24 export, mouse anti-HA (1:500), rabbit anti-inner membrane complex 1 (IMC1, 1:500, available in our laboratory), goat anti-mouse IgG (H+L) conjugated with Alexa Fluor 488 (1:500, Thermo Fisher Scientific, USA), goat anti-rabbit IgG (h + L) conjugated with Alexa Fluor 594 (1:500, Thermo Fisher Scientific, USA) and DAPI were used for the IFA (Mayoral et al., 2020). To assess cyst conversion, rabbit anti-IMC1 and FITC-DBA were used to detect the parasites and cyst walls, respectively.

2.9. Plaque assays

Confluent HFF monolayers grown in 12-well plates were infected with 500 tachyzoites of wild-type, Δ*gra76* or Δ*gra76*C per well, and the plates were incubated for seven or 12 days (Zheng et al., 2023). After incubation, the cells were washed with PBS prior to fixation with 4% PFA for 20 min. Then, 0.2% crystal violet (Solarbio, China) was used to stain the HFFs for 20 min, followed by two washes with PBS. The plaques were imaged and quantified using ImageJ software.

2.10. Assessment of parasite replication, egress and invasion

To investigate the intracellular replication efficiency of the parasites, 10^5 tachyzoites per well were used to infect HFF monolayers for 1 h prior to washing with DMEM. After 24 h incubation, IFAs with mouse anti-SAG1 (1:500) and Alexa Fluor 488 goat-anti mouse IgG (H+L) were performed to visualize and count the number of tachyzoites in at least 100 PVs (Liang et al., 2021). For egress assays, 2×10^4 parasites were cultured for 32-36 h before adding 3 μM calcium ionophore A23187 (Abcam, UK) in DMEM to induce parasite egress at 37 °C for 2 min. The samples were fixed immediately with 4% PFA, and an IFA was performed using rabbit anti-GAP45 (1:500) to stain the parasite (Liang et al., 2021). The numbers of both intact and egressed PVs were counted, and the number of egressed PVs relative to the total number of PVs was used to calculate the egress efficiency. To examine the invasion ability of different strains, 2×10^6 freshly egressed tachyzoites per well were allowed to infect HFF monolayers at 37 °C for 30 min. Subsequently, samples were gently washed with PBS to remove unbounded tachyzoites (Li et al., 2021). An IFA was used to stain the extracellular tachyzoites with mouse anti-SAG1 (1:500) and Alexa Fluor 594 goat-anti mouse IgG (H+L). The extracellular and intracellular tachyzoites were stained with rabbit anti-IMC1 antibody and Alexa Fluor 488 goat-anti rabbit IgG (H+L) after permeabilization with 0.2% Triton X-100. At least 20 fields were quantified per sample to calculate the proportion of intracellular tachyzoites/total tachyzoites. Three independent experiments for each assay were performed.

2.11. Effect of GRA76 on trafficking of GRA16 and GRA24

To evaluate the role of GRA76 in the trafficking of secretory GRA proteins, the epitopic expression plasmids were transiently transfected into *T. gondii* parasites (Gold et al., 2015). For construction of epitopic expression plasmids, the coding sequence of GRA16 or GRA24, which was amplified from the cDNA using specific primers with overhangs to pGRA1-3HA-CAT sequence, were fused with the pGRA1-3HA-CAT plasmid backbone. The epitopic expression vectors (pGRA1-GRA16-3HA-CAT or pGRA1-GRA24-3HA-CAT) were transiently transfected into the RH, RHΔ*gra76*, RHΔ*gra76*C, Pru, PruΔ*gra76* or PruΔ*gra76*C tachyzoites using electroporation. After 24 h infection of HFFs, tachyzoites were examined for export of the epitopically expressed GRA16 or GRA24 using an IFA. At least 30

infected host cells containing a single PV with two or more parasites were observed (Cygan et al., 2020, Mayoral et al., 2020). Primers used are listed in Supplementary Table S1.

2.12. The effect of gra76 deletion on global gene expression

To gain insight into the expression of genes affected by *gra76* deletion, global transcriptome profiling was performed to identify the differentially expressed genes between PruΔ*gra76* and the wild-type Pru strain, using RNA-Seq. Tachyzoites of PruΔ*gra76* and Pru were allowed to infect HFF monolayers for 45 h (Pru strain) or 3 days (PruΔ*gra76* strain) to obtain comparable numbers of parasites per vacuole. Then, infected monolayers were washed twice with PBS, scraped off, and centrifuged at 300 *g* for 15 min. Three independent samples were prepared from each strain. Total RNA of each sample was extracted using the TRIzol method and the residual genomic DNA was removed with RNase-Free DNase (Thermo Fisher Scientific, USA). The quantity and quality of total RNA in each sample were examined using a Nano Drop and Agilent 2100 bioanalyzer (Thermo Fisher Scientific, USA). The library was constructed following a series of steps including mRNA isolation, mRNA fragmentation, cDNA synthesis, cDNA modification, PCR and the clean-up using AMPure XP beads (Beckman Coulter, USA) (Wang et al., 2022). Sequencing of the RNA libraries was performed using the BGI-AEQ platform (Shenzhen, China). The raw reads were trimmed and filtered using SOAPnuke to remove reads containing sequencing adapter, with a low-quality base ratio (> 20%) or with > 5% unknown base ratio (Li et al., 2008). The trimmed reads were aligned to the *T. gondii* ME49 genome (https://toxodb.org/toxo/app) using hierarchical indexing for spliced alignment of transcripts (HISAT) (Kim et al., 2015). The relative gene expression was calculated by the fragments per kilobase of exon model per million mapped fragments (FPKM) method using RSEM (v1.3.1) (Li and Dewey, 2011). Data mining was performed on the Dr. Tom Multi-omics Data mining system (https://biosys.bgi.com). The differential expression analysis was performed using DESeq2 (v1.4.5) (Love et al., 2014), and a gene with a $\log_2$ fold change of ≥ 1 or ≤ -1 and Q value (adjusted *P* value) of ≤ 0.05 was considered significant.

2.13. Real time quantitative PCR (RT-qPCR)

The expression of 10 randomly selected genes (seven upregulated genes and three downregulated genes) in RNA samples were analyzed by real time quantitative PCR (RT-qPCR) on a LightCycler 480 PCR platform (Roche, Basel, Switzerland) to validate gene expression changes obtained by RNA-Seq. The RT-qPCR was conducted as described previously (Zheng et al., 2021), and expression of the target genes was normalized to that of *β*-tubulin. Each sample was independently analyzed three times.

2.14. Virulence in mice

Mice were intraperitoneally (ip) injected with 1×10^2 tachyzoites of RH, RHΔ*gra76* or RHΔ*gra76*C, or two doses (2×10^2 and 5×10^4) of Pru, PruΔ*gra76*, PruΔ*gra76*C and PruΔ*gra76*C_{Tub} tachyzoites. Six mice were used for each infection dose or strain. The number of viable tachyzoites for each strain used to infect mice was quantified by plaque assays to ensure the tachyzoites used in animal infection were viable (Franco et al., 2016). The clinical signs and survival of the infected mice were observed twice daily for 30 days. Mice were euthanized immediately when they reached their humane endpoint. At 30 days p.i., brains of the mice which survived Pru or PruΔ*gra76* infection were collected and homogenized. The number of brain cysts was counted as previously described (Wang et al., 2017, Wang et al., 2020a).

2.15. Immune protection against T. gondii infection by PruΔgra76 vaccination

Mice were immunized with 5×10^4 PruΔ*gra76* tachyzoites. At 45 days p.i., serum samples of naive and immunized mice were collected to detect the levels of anti-*T. gondii* total IgG and subclasses IgG1 and IgG2a antibodies using ELISA (Liang et al., 2020, Wang et al., 2020b). The naive and immunized mice were challenged ip with 1×10^3 RH tachyzoites or 1×10^3 PYS (ToxoDB#9, Chinese I) tachyzoites to examine protection against acute infection. To investigate the protective efficacy against chronic infection, immunized and naive mice were orally administered 10 or 40 Pru cysts at 45 days after immunization. Clinical signs and survival of infected mice were observed twice daily up to 30 days post-reinfection. To determine the brain cyst burden, the number of brain cysts was counted in the naive and vaccinated mice that remained alive 30 days p.i. as previously described (Wang et al., 2017).

2.16. Statistical analysis

Statistical analyses were performed using GraphPad Prism software (version 9.0). All data were analyzed based on three independent experiments. The results shown are the means ± standard deviations (S.D.). The significant difference between two groups or ≥ 3 groups was determined by two-tailed, unpaired Student *t* test, or one-way ANOVA, respectively. The difference between groups was considered statistically significant when the *P* values were < 0.05.

3. Results

3.1. Characterization of the novel GRA76

The GRA76 protein contains 545 amino acids and has a predicted signal peptide and three transmembrane domains proximal to the C terminus (Supplementary Fig. S1A). Using PONDR (http://www.pondr.com), GRA76 was predicted to contain five regions of protein intrinsically

disordered regions (IDR), which are abundant in most GRAs and other secreted effector proteins in bacteria (Nyonda et al., 2021, Rosenberg and Sibley, 2021) (Supplementary Fig. S1B). The presence of IDR in GRA76 suggests a flexible structure and a high possibility of promiscuous interaction with other proteins. Three transmembrane domains at amino acids 372-391, 438-455 and 475-497 were predicted in GRA76 by TMHMM (Supplementary Fig. S1C). The first 28 amino acids in the N terminus of GRA76 were predicted as a signal peptide using SignalIP 5.0 (Supplementary Fig. S1D). Consistent with most GRAs, GRA76 did not have any homology to other eukaryotic proteins and we did not detect any homology to any other known functional protein domain or site.

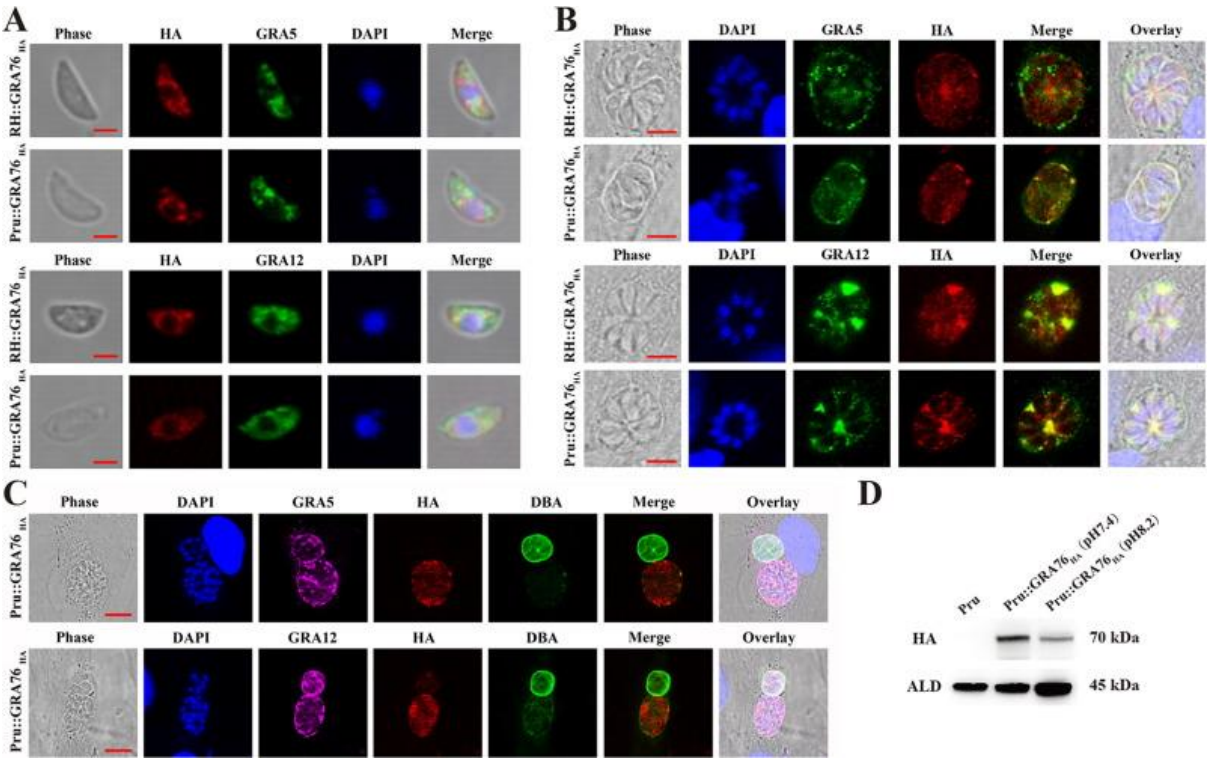

Fig. 1. The newly characterized GRA76 dense granular protein is highly expressed in tachyzoites, and mainly localized to the parasitophorous vacuole (PV) of *Toxoplasma gondii*. (A) Immunofluorescence assay (IFA) of extracellular parasites showing GRA76 localized to the dense granules, as indicated by partly co-localizing with GRA5 or GRA12 in RH and Pru strains. Extracellular tachyzoites were stained with GRA5 or GRA12 antibodies (green), hemagglutinin (HA) antibodies (red) and DAPI (blue). Scale bars = 2 μm. (B) Subcellular localization of GRA76 in the intracellular tachyzoites of *T. gondii* RH and Pru strains. Cells infected with tachyzoites expressing HA-tagged GRA76 in RH or Pru strain were stained with GRA5 or GRA12 antibodies (green), HA antibodies (red) and DAPI (blue) 24 h p.i. GRA76 protein was partly co-localized with GRA5 and GRA12 in intracellular tachyzoites of *T. gondii*. Scale bars = 5 μm. (C) Subcellular localization of GRA76 in the bradyzoites of *T. gondii* Pru strain. Parasites were stained with HA antibodies (red), GRA5 or GRA12 (magenta), FITC-*Dolichos Biflorus* agglutinin (FITC-DBA) (green) and DAPI (blue) after 48 h post-differentiation. The expression of GRA76 was almost undetectable in the bradyzoites (DBA-positive vacuole). Scale bars = 10 μm. (D) Representative

western blot images probed with anti-HA to detect the levels of HA-tagged GRA76 protein of Pru strain in a normal culture medium (pH 7.4) and in an alkaline culture medium (pH 8.2). The expression level of the tagged protein in tachyzoites was higher than that in bradyzoites. Aldolase (ALD) was used as a loading control. All experiments were performed three independent times. RH, *Toxoplasma* wild-type I strain. Pru, *Toxoplasma* wild-type II strain. RH::GRA76$_{HA}$, *Toxoplasma* RH strain in which GRA76 was tagged with HA epitope. Pru::GRA76$_{HA}$, *Toxoplasma* Pru strain in which GRA76 was tagged with HA epitope.

3.2. GRA76 is expressed more in the tachyzoite stage than in the bradyzoite stage

To determine the subcellular localization of GRA76, a six C-terminal HA epitope tag (6 × HA) was appended to the endogenous gene, immediately after the STOP codon using CRISPR-Cas9 mediating homologous recombination in RHΔ*ku80* and PruΔ*ku80* strains (Supplementary Fig. S2A). The integration was confirmed by PCR, sequencing, and western blots (Supplementary Fig. S2B-D). Western blots analysis of the protein extracted from the extracellular parasites of GRA76::HA line revealed an approximately 70 kDa band which matched the predicted size of the full protein (60 kDa) plus six copies of HA (approximately 10 kDa) (Supplementary Fig. S2D).

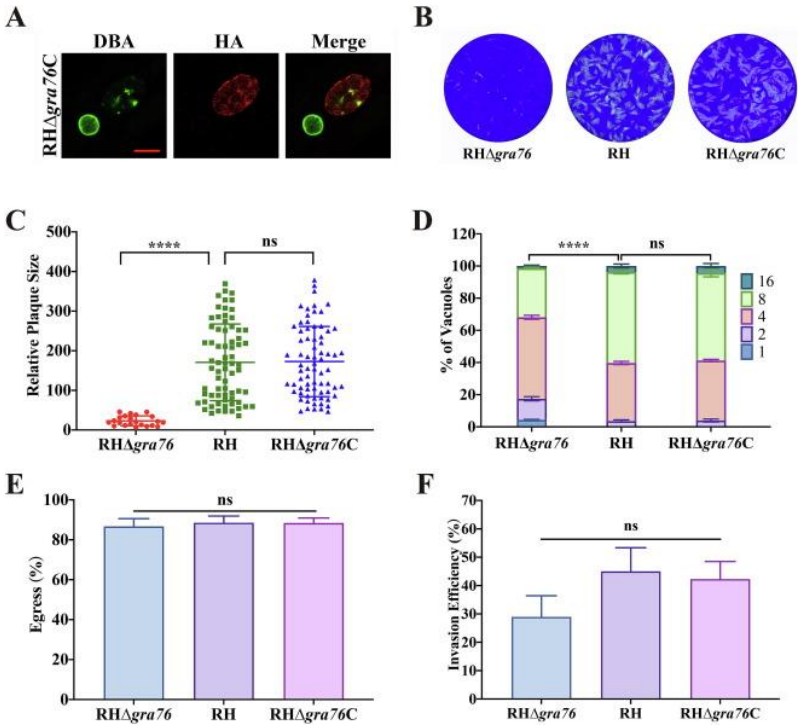

Fig. 2. GRA76 dense granule protein is involved in the growth of *Toxoplasma gondii* RH strain tachyzoites in vitro. (A) Immunofluorescence assay (IFA) shows that the parasite stage differential expression characteristic of GRA76 was complemented in RHΔ*gra76*C. Scale bars = 10 μm. (B) Representative images of three independent plaque assays in which the plaques were formed by RH, RHΔ*gra76* and RHΔ*gra76*C tachyzoites in human foreskin fibroblasts (HFFs) 7 days p.i. (C) Analysis of the relative size and number of the plaques (B) shows that deletion of *gra76* significantly decreased

the plaque formation of RH tachyzoites in vitro (****$P < 0.0001$). The data are presented as mean ± S.D. of each plaque area in B, showing one comparable representative image from three independent experiments. (D) Intravacuolar replication of the indicated strains was determined by counting the number of parasitophorous vacuoles (PVs) containing one, two, four, eight, and 16 tachyzoites, 24 h p.i. The intracellular replication of RHΔ*gra76* tachyzoites was significantly lower compared with RH and RHΔ*gra76*C tachyzoites (****$P < 0.0001$), indicating that GRA76 contributes to the intracellular replication of RH tachyzoites. (E) The egress capacity of RHΔ*gra76* tachyzoites showed no marked difference compared with RH or RHΔ*gra76*C strains. (F) No significant difference was detected in tachyzoite invasion efficiency between RHΔ*gra76* and RH or RHΔ*gra76*C. All results were based on three independent experiments. ns, not significant. RH, *Toxoplasma* wild-type I strain. RHΔ*gra76*, *Toxoplasma* knockout strain which lost *gra76* gene in RH strain. RHΔ*gra76*C, *Toxoplasma* complemented strain which was complemented with wild-type *gra76*gene driven by its own promoter in RHΔ*gra76* strain.

Results of the IFA showed that GRA76 was partly co-localized with the GRA markers GRA5 and GRA12 in the extracellular tachyzoites of both type I RH and type II Pru strains (Fig. 1A). In the intracellular tachyzoites, GRA76 was mainly secreted into the PV and partly co-localized with GRA5 and GRA12 (Fig. 1B), indicating that GRA76 was localized to the dense granules. To assess whether GRA76 was associated with the cyst wall in bradyzoites, the same as most GRAs, tachyzoites were induced to differentiate into bradyzoites in a differentiation medium (pH = 8.2) and ambient CO_2 environment for 2 days. Interestingly, the presence of the HA stain was scarcely detected in the cysts containing bradyzoites that were positive for DBA staining. However, it was observable in vacuoles that were negative for DBA staining (Fig. 1C), suggesting that the expression of GRA76 was higher in the tachyzoite satge compared to the bradyzoite stage. The stage-differential expression of GRA76 was verified by western blots of the Pru::GRA76-HA strain cultured under normal condition for 3 days and differentiation conditions for 7 days (Fig. 1D).

3.3. GRA76 is important for the in vitro growth of both RH and Pru tachyzoites

To investigate whether GRA76 plays a role in the *in vitro* growth of the *T. gondii* RH strain, *gra76* was disrupted using CRISPR-Cas9. The parental strains were co-transfected with the CRISPR plasmid targeting *gra76* and the fragments of a DHFR drug-selective marker with homologous arms of *gra76* (Supplementary Fig. S3A). After selection with pyrimethamine, single clones were isolated and tested by PCRs (Supplementary Fig. S3A). The successful disruption of *gra76* was verified by PCR, where the coding sequence of *gra76* was not amplified in the mutant strains but was detected in the wild-type RH strain as shown by PCR4, and two recombinational sequences were amplified in *gra76*knockout strains but not in the RH strains as shown by PCR3 and PCR5 (Supplementary Fig.

S3B). To ensure that the changed phenotype is attributed to the loss of *gra76*, RHΔ*gra76* was complemented by adding a C-terminal 3 × HA tagged wild-type copy of *gra76* into the HXGPRT locus (Supplementary Fig. S3C). The integration of *gra76* coding sequence into the HXGPRT locus in the complemented strain (RHΔ*gra76*C) was verified by PCRs (Supplementary Fig. S3D), IFA analysis (Fig. 2A, Supplementary Fig. S3E), and western blots (Supplementary Fig. S3F). IFA also showed that the differential expression characteristic of GRA76 in RHΔ*gra76*C was the same as that observed in the wild-type strain (Fig. 2A).

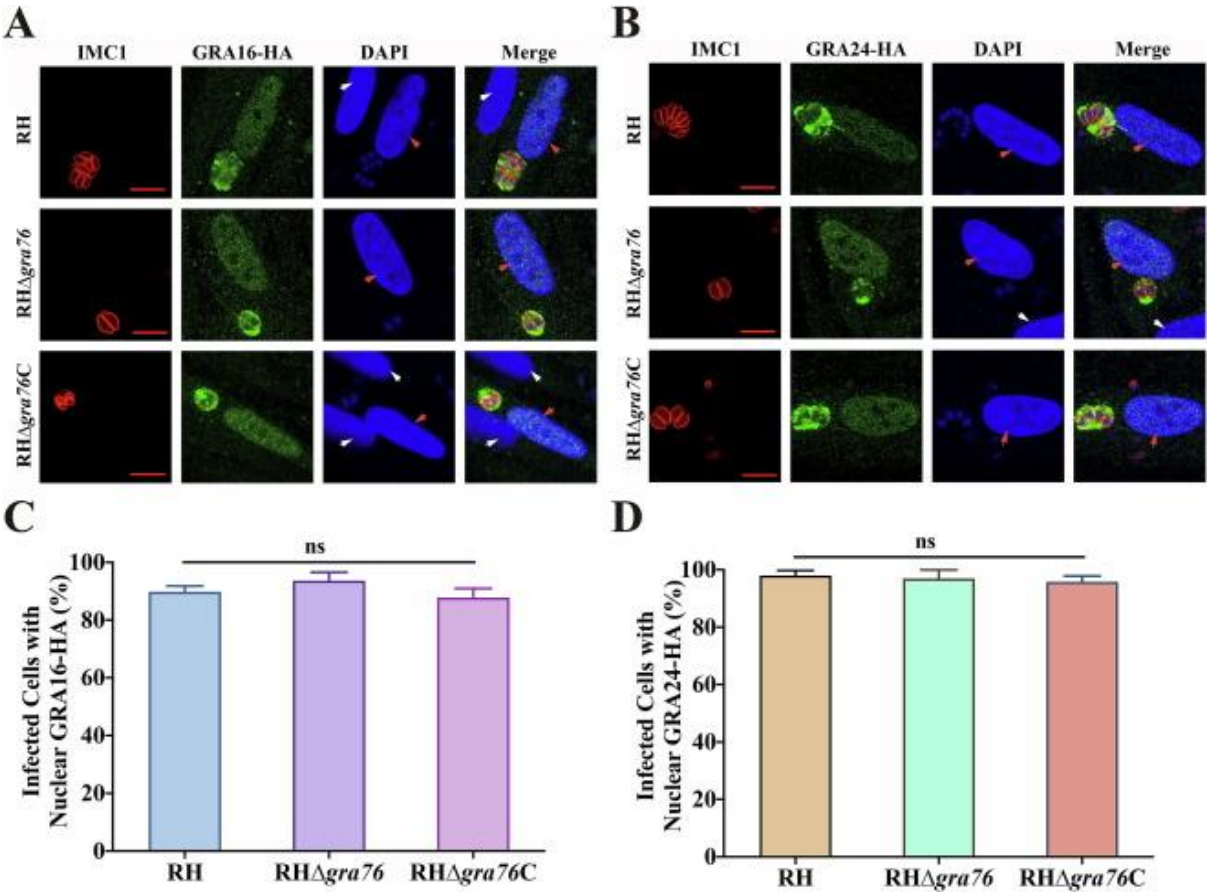

Fig. 3. Disruption of dense granule protein GRA76 gene (*gra76*) has no impact on the trafficking of GRA16 and GRA24 dense granular proteins in *Toxoplasma gondii* RH strain. Representative immunofluorescence images of RH-, RHΔ*gra76*- and complemented RHΔ*gra76* (RHΔ*gra76*C)-infected human foreskin fibroblasts (HFFs) cells stained with inner membrane complex 1 (IMC1) antibody to detect parasites (red), DAPI to detect DNA (blue) and hemagglutinin (HA) antibody to detect GRA16 or GRA24 (green). The localization of GRA16 (A) and GRA24 (B) in RHΔ*gra76* strain was the same as that observed in wild-type RH and the complemented RHΔ*gra76*C strains. The white arrows denote the nuclei of the uninfected host cells, and the red arrows denote the infected cells. Scale bars = 10 μm. Percentages of infected cells with GRA16 (C) and GRA24 (D) localization in the host nucleus based on three independent experiments. At least 30 host cells containing a single parasitophorous vacuole with two or more parasites were observed. ns, not significant. GRA, dense granular protein. RH, *Toxoplasma* wild-type I strain. RHΔ*gra76*, *Toxoplasma* knockout strain which

lost *gra76* gene in RH strain. RHΔ*gra76*C, *Toxoplasma* complementened strain which was complemented with wild-type *gra76* gene driven by its own promoter in RHΔ*gra76* strain.

To investigate the role of GRA76 in the growth of RH tachyzoites in vitro, a standard plaque assay was performed. The results showed that deletion of *gra76* in the RH strain significantly reduced plaque formation as was shown by a significant reduction in the size and number of plaques in confluent HFFs formed 7 days p.i., compared with plaques fromed by the wild-type strain ($P < 0.0001$, Fig. 2B and C). Plaque assays comprehensively evaluate the lytic cycle progression, including tachyzoite invasion, intracellular growth, and egress (Blume et al., 2009). To determine which part of the lytic cycle was affected by the disruption of *gra76*, intracellular replication, egress efficiency and invasion assays were performed. RHΔ*gra76* showed a significant reduction in intracellular replication at 24 h p.i. ($P < 0.0001$, Fig. 2D). However, neither the egress nor invasion efficiency was affected in RHΔ*gra76* ($P > 0.05$, Fig. 2E and F). The complemented strain (RHΔ*gra76*C) rescued the defect in RHΔ*gra76*. To determine whether the function of GRA76 is strain-specific, we deleted the *gra76* gene in the type II Pru strain and complemented the protein in PruΔ*gra76* (PruΔ*gra76*C, Supplementary Fig. S4A-D and G-J). The results of plaque assays observed for the PruΔ*gra76* strain were similar to those obtained with RHΔ*gra76* (Supplementary Fig. S4E and F), suggesting that GRA76 is important for parasite intracellular replication in the type I RH strain and type II Pru strain.

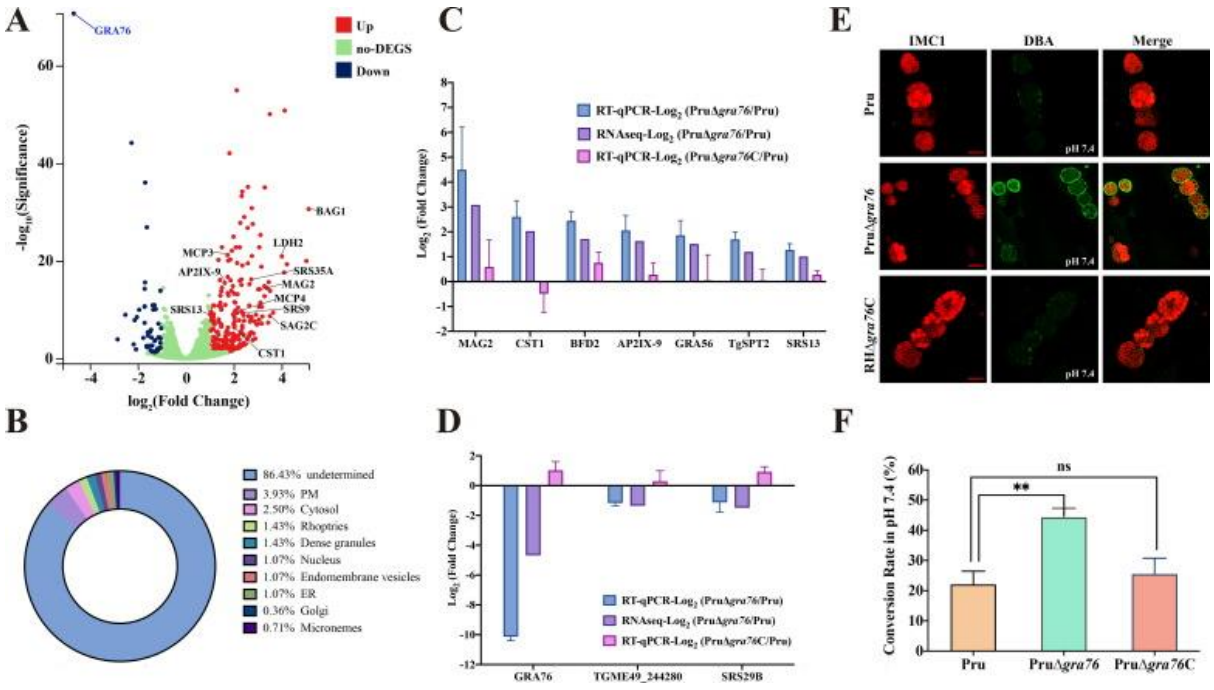

Fig. 4. Loss of GRA76 dense granular protein in *Toxoplasma gondii* Pru strain increases the expression of bradyzoite-associated genes and significantly increases bradyzoite conversion in vitro. (A) Volcano plot showing the transcriptional profile of PruΔ*gra76*compared with the wild-type Pru. Bradyzoite-associated genes were up-regulated in PruΔ*gra76*. (B) Pie graph showing the predicted localization of the differentially up-regulated proteins in PruΔ*gra76*. Predicted localization of *T. gondii* proteins was

obtained from ToxoDB (https://toxodb.org). (C-D) Expression verification of the randomly selected up-regulated genes (C) and down-regulated genes (D) by real time quantitative PCR (RT-qPCR). (E) Representative immunofluorescence images of vacuoles formed by the indicated strains under normal culture conditions (pH 7.4) for 48 h. The vacuoles were stained by *Dolichos Biflorus* agglutinin (DBA) (green) or inner membrane complex 1 (IMC1) antibody (red). Scale bar = 10 μm. (F) The percentages of DBA-positive cysts of indicated strains calculated based on counting at least 100 vacuoles per sample in three independent experiments. Pru, *Toxoplasma* wild-type II strain. Pru*Δgra76*, *Toxoplasma*knockout strain which lost *gra76* gene in Pru strain. Pru*Δgra76*C, *Toxoplasma*complementened strain which was complemented with wild-type *gra76* gene driven by its own promoter in Pru*Δgra76* strain.

3.4. GRA76 is not required for trafficking of GRA16 and GRA24 to the host nucleus.

To test whether GRA76 plays a role in the export of GRAs across the PVM, the localization of GRA16 or GRA24 in the RH, RH*Δgra76*, RH*Δgra76*C, Pru, Pru*Δgra76* and Pru*Δgra76*C strains was compared. We constructed plasmids expressing a C-terminal HA-tagged version of GRA16 or GRA24 driven by GRA1 promoter. The plasmids were transfected into the extracellular tachyzoites of RH, RH*Δgra76*, RH*Δgra76*C, Pru, Pru*Δgra76* and Pru*Δgra76*C strains, which were then used to infect HFFs for 24 h. GRA16-HA or GRA24-HA was visualized using IFAs. The results revealed that the host nucleus localization levels of GRA16 and GRA24 in RH*Δgra76* and Pru*Δgra76* were equivalent to those observed in RH, RH*Δgra76*C, Pru and Pru*Δgra76*C strains (Fig. 3 and Supplementary Fig. S5), suggesting that GRA76 is not necessary for the translocation of GRA16 and GRA24 across the PVM to the host cell nucleus.

3.5. Deletion of gra76 upregulates bradyzoite-associated genes and increases bradyzoite formation

We examined whether disruption of *gra76* influences the global expression of *T. gondii*genes. RNAs were isolated from intracellular tachyzoites of Pru*Δgra76* and wild-type Pru cultured under normal culture conditions for RNA-seq analysis. A differential expression profile in Pru*Δgra76* was identified using a $\log_2$ fold change of ≥ 1 or ≤ -1, and Q values (adjusted *P* values) ≤ 0.05. This analysis revealed large differences in gene expression between the Pru*Δgra76* strain and the wild-type Pru strain. Compared with the wild-type Pru strain, 198 genes were up-regulated (≥ 2-fold), and 47 genes were down-regulated (≤ -2-fold) in the Pru*Δgra76* strain (Fig. 4A and Supplementary Tables S2-S4). However, localization of the most upregulated proteins in Pru*Δgra76* was not predicted (160/198, Fig. 4B), according to the spatial data obtained from hyperLOPIT analysis (Barylyuk et al., 2020). The expression changes of 10 randomly selected differentially expressed genes were confirmed by RT-

qPCR (Fig. 4C and D). The results also showed that the expression changes of the up-regulated or down-regulated genes in PruΔ*gra76* were restored in PruΔ*gra76*C (Fig. 4C and D).

The expressions of bradyzoite-associated genes were significantly up-regulated in PruΔ*gra76* tachyzoites, including BAG1 (Bohne et al., 1995), MAG2 (Tu et al., 2020a), ENO1 (Kibe et al., 2005), LDH2 (Yang and Parmley, 1997, Abdelbaset et al., 2017), AP2IX-9 (Radke et al., 2013, Hong et al., 2017) and CST1 (Tomita et al., 2013) (Fig. 4A), indicating GRA76 maybe involve in bradyzoite differentiation. To investigate whether *gra76*knockout increased propensity for bradyzoite formation in vitro, we evaluted the bradyzoite conversion rate of Pru, PruΔ*gra76* and PruΔ*gra76*C tachyzoites under normal culture conditions. The results showed that PruΔ*gra76* tachyzoites had significantly increased propensity for forming bradyzoites, compared with tachyzoites of the Pru and complemented PruΔ*gra76*C strains (Fig. 4E and 4F). Together, these results indicate that inactivation of GRA76 causes up-regulation of genes involved in tachyzoite-to-bradyzoite differentiation and increases bradyzoite conversion.

3.6. GRA76 is important for parasite virulence and cyst burden

Because GRA76 is important for in vitro fitness of *T. gondii*, we investigated the contribution of GRA76 to parasite virulence in vivo by ip injection of Kunming mice with either type I or type II Δ*gra76* tachyzoites. The survival of mice was monitored for 30 days p.i. In the case of type I tachyzoite infection, mice infected with 100 RH tachyzoites survived for a median of 9 days before they reached the humane endpoint criteria, while mice infected with the same dose of RHΔ*gra76* tachyzoites exhibited a median of 13 days (Fig. 5A). The survival difference between the two groups was significant ($P<0.01$). Importantly, the virulence defect of RHΔ*gra76* was rescued by GRA76 complementation (Fig. 5A). To examine the effect of GRA76 on the parasite virulence during type II tachyzoite infection, mice were infected with different doses of Pru and PruΔ*gra76*tachyzoites. Interestingly, the survival rates of mice infected with the two infectious doses of PruΔ*gra76* tachyzoites were 100% at 30 days p.i. (Fig. 5B and C). In contrast, all mice infected by Pru tachyzoites reached their humane endpoint criteria, except 37.5% of mice infected with the lower dose (2×10^2) of Pru tachyzoites (Fig. 5B and C). The survival rates of the PruΔ*gra76*-infected groups were significantly higher than the survival rates of the Pru-infected groups. No clinical signs were observed in 2×10^2 and 5×10^4 PruΔ*gra76*-infected mice. We also compared the virulence of two complemented strains, PruΔ*gra76*C and PruΔ*gra76*C_{Tub}, at two doses of infection (2×10^2 and 5×10^4tachyzoites). The defect in the virulence of PruΔ*gra76* was rescued in PruΔ*gra76*C but not in PruΔ*gra76*C_{Tub} (Fig. 5B and C). This result may be attributed to the differential stage expression patterns of GRA76 between PruΔ*gra76*C and PruΔ*gra76*C_{Tub} (Supplementary Fig. S4D, I and J). To assess the cyst forming ability of GRA76, the brain cyst numbers of the surviving mice were determined at 30 days p.i. The results showed

that *gra76*deletion caused a marked reduction in parasite cyst burden in the PruΔ*gra76*-infected group compared with the Pru-infected group (Fig. 5D).

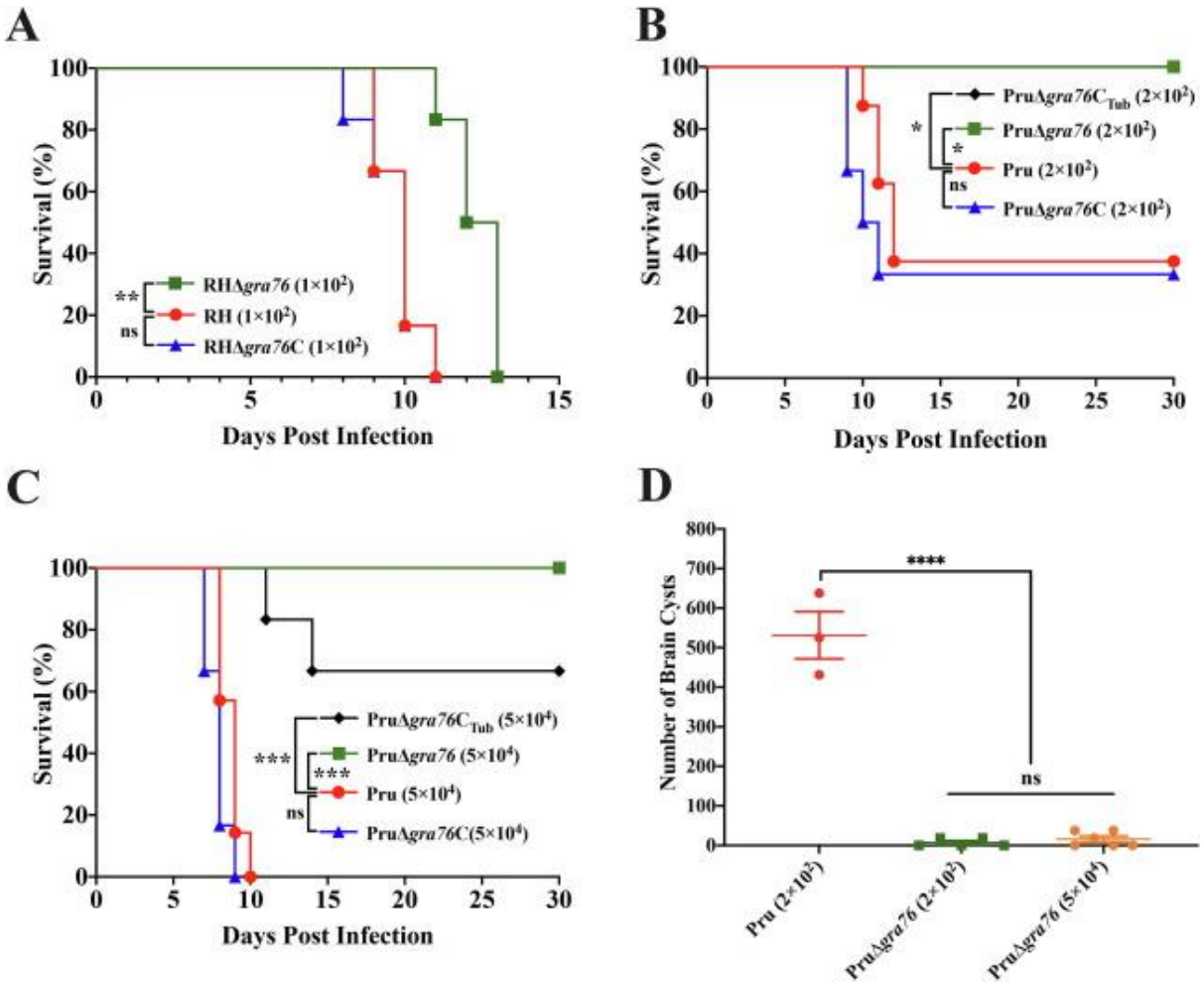

Fig. 5. Deletion of dense granule protein GRA76 gene (*gra76*) significantly attenuates the *Toxoplasma gondii* parasite virulence and reduces brain cyst formation in vivo. Female Kunming mice were intraperitoneally infected with tachyzoites of the indicated doses or strains and were monitored for 30 days. Statistical significance was tested by a Log rank Mantel-Cox test. (A-C) Survival curve of mouse groups that received the following doses of tachyzoites: 1×10^2 tachyzoites of RHΔ*gra76*, RH or complemented RHΔ*gra76*(RHΔ*gra76*C) (A, $^{**}P = 0.0015$), 2×10^2 (B, $^{*}P = 0.0226$) or 5×10^4 (C, $^{***}P = 0.0004$) tachyzoites of PruΔ*gra76*, Pru, PruΔ*gra76*C, or PruΔ*gra76*C_{Tub} strains. (D) Brain cyst burden of the surviving mice ($^{****}P < 0.0001$, unpaired test). The number of brain cysts in PruΔ*gra76*-infected group was significantly lower than that of the Pru-infected group. RH, *Toxoplasma* wild-type I strain. RHΔ*gra76*, *Toxoplasma* knockout strain which lost *gra76* gene in RH strain. RHΔ*gra76*C, *Toxoplasma* complemented strain which was complemented with wild-type *gra76* gene driven by its own promoter in RHΔ*gra76*strain. Pru, *Toxoplasma* wild-type II strain. PruΔ*gra76*, *Toxoplasma* knockout strain which lost *gra76* gene in Pru strain. PruΔ*gra76*C, *Toxoplasma* complemented strain which was complemented with wild-type *gra76* gene driven by its own promoter in PruΔ*gra76*strain. PruΔ*gra76*C_{Tub}, *Toxoplasma* complementened strain

which was complemented with wild-type *gra76* gene driven by the *Toxoplasma* tubulin promoter in PruΔ*gra76*strain.

3.7. PruΔgra76 vaccination partly protects mice against T. gondii infection

Considering the significantly attenuated virulence of PruΔ*gra76* in mice, we tested the potential protection conferred by immunization using PruΔ*gra76* against *T. gondii* infection. An infection dose of 5 × 10^4 PruΔ*gra76* tachyzoites produced a small number of brain cysts (median = 16 ± 18 cysts) (Fig. 5D) and therefore was selected for vaccination. To examine the protective efficacy of PruΔ*gra76* immunization against acute infection, mice were vaccinated with 5 × 10^4 PruΔ*gra76* tachyzoites. No clinical signs were observed in the immunized mice. At 45 days post-vaccination, the immunized and naive mice were challenged with 10^3 tachyzoites of RH strain or PYS strain. The vaccinated mice challenged with 10^3 RH tachyzoites had a better survival than naive mice (Fig. 6A). The survival rate of the vaccinated mice challenged with 10^3 PYS tachyzoites was 100%, whereas all the naive mice reached their humane endpoints after 10 days (Fig. 6B). These results indicate that live-attenuated PruΔ*gra76*-based vaccination confers partial protection against acute *T. gondii* infection by PYS and RH strains.

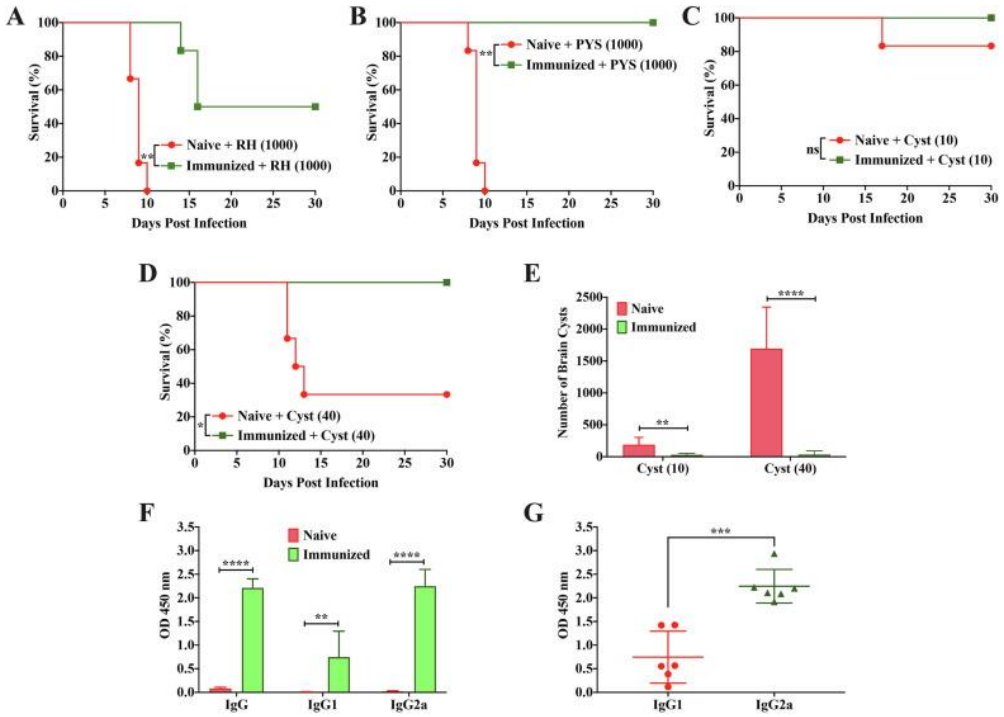

Fig. 6. Vaccination with *Toxoplasma gondii* PruΔ*gra76* tachyzoites protects mice against acute and chronic *T. gondii* infections. (A-B) Kunming mice were immunized with 5 × 10^4PruΔ*gra76* tachyzoites and then the immunized and naive mice were intraperitoneally challenged by 1 × 10^3 RH strain tachyzoites (A) or 1 × 10^3 PYS strain (ToxoDB#9, Chinese I) tachyzoites at 45 days post-vaccination (B). Survival was monitored for an additional 30 days (six mice/strain). (C-D) The immunized and naive mice were orally challenged by 10 cysts (C) or 40 cysts (D) at 45 days post-vaccination. Naive

mice were considered negative controls. The survival percentage of immunized mice was significantly higher than that of naive mice in each group. (E) Brain cyst burden in the chronically infected mice. Vaccination with PruΔ*gra76* significantly reduced the number of brain cysts in mice. (F) Levels of anti-*T. gondii*-specific total IgG and IgG subclass (IgG1 and IgG2a) antibodies in the serum of mice at 45 days post-vaccination. A remarkable increase in the level of total IgG, IgG1 and IgG2a was induced by PruΔ*gra76* vaccination. (G) The IgG2a level was significantly higher than that of IgG1 in the PruΔ*gra76*-immunized mice. ****P< 0.0001 ***P < 0.001, **P < 0.01. RH, *Toxoplasma* wild-type I strain. PruΔ*gra76, Toxoplasma*knockout strain which lost *gra76* gene in Pru strain.

To assess the protective efficacy of PruΔ*gra76* immunization against chronic infection, the vaccinated and naive mice were orally challenged with 10 and 40 cysts of the Pru strain at 45 days post-vaccination. The survival rate in PruΔ*gra76*-vaccinated mice challenged with 10 or 40 Pru cysts was 100%, while that of the naive mice challenged with 10 and 40 Pru cysts was 83% and 33%, respectively (Fig. 6C and D). At 30 days p.i., the brain cyst burden was determined in the surviving mice. The numbers of brain cysts in vaccinated mice were significantly decreased compared with those of naive mice (Fig. 6E). An approximately similar number of cysts was detected in immunized mice challenged with two different doses (29 ± 25 cysts in mice challenged with 10 cysts and 32 ± 61 cysts in mice challenged with 40 cysts), suggesting that these cysts are produced by PruΔ*gra76* vaccination and that PruΔ*gra76* vaccination was effective at preventing the challenge doses of the wild-type Pru cysts from establishing new cysts.

3.8. PruΔgra76 vaccination induces a Th1-biased immune response

To elucidate the factors that mediate the protective immune response conferred by PruΔ*gra76* vaccination, serum samples were collected from immunized and naive mice at 45 days post-vaccination. The levels of anti-*T. gondii* IgG and subclasses (IgG1 and IgG2a) were measured by ELISA (Liang et al., 2020, Wang et al., 2020b). Significantly increased levels of IgG were observed in the vaccinated group (Fig. 6F). The levels of IgG1 and IgG2a antibodies were also significantly increased in the vaccinated mice (Fig. 6F), and the level of IgG2a was significantly higher than that of IgG1 (Fig. 6G), indicating that PruΔ*gra76*vaccination induced a Th1-biased immune response to counter intracellular *T. gondii* infection.

4. Discussion

To survive and propagate inside the host cells, *T. gondii* secretes different effector proteins to control host cell machinery (Clough and Frickel, 2017, Hakimi et al., 2017, Wang et al., 2020d). One important group of those effectors is GRAs, secreted from the dense granule organelle. GRAs with different localizations play important roles in host cell immune suppression, PV and PVM modification, nutrient

acquisition and cyst formation (Hakimi et al., 2017, Jeffers et al., 2018, Wang et al., 2020d). However, the biological functions of many putative GRAs have not been fully elucidated (Barylyuk et al., 2020, Tu et al., 2020b). The data presented here show that GRA76 is important for the growth and virulence of *T. gondii*.

In the present study, subcellular localization of GRA76 in tachyzoites and bradyzoites was investigated. Interestingly, the expression level of GRA76 in tachyzoites was higher than that in bradyzoites, consistent with the transcriptomics dataset in ToxoDB (https://toxodb.org) (Buchholz et al., 2011, Fritz et al., 2012, Pittman et al., 2014). In tachyzoites, GRA76 partly co-localized with GRA5 and GRA12, in agreement with that of most GRAs (Barylyuk et al., 2020, Wang et al., 2020d, Zheng et al., 2023). The expression pattern of GRA76 differs from the majority of known GRAs, which are continuously expressed in both tachyzoites and bradyzoites, or mainly in bradyzoites (Jeffers et al., 2018, Zheng et al., 2023). The expression pattern of GRA76 was governed by its own promoter because stage-differential expression characteristics were not restored in PruΔ*gra76*C_{Tub}, where GRA76 was under the control of a *Toxoplasma* tubulin promoter, but were restored in PruΔ*gra76*C when GRA76 was driven by its own promoter.

In the present study, we found that a *gra76*-deficient mutant did not show any significant defect in egress and invasion, suggesting that GRA76 was not necessary for tachyzoite egress and invasion, similar to most of the known GRAs (Bai et al., 2018, Griffith et al., 2022, Zheng et al., 2023). However, deleting *gra76* resulted in a significant reduction in plaque formation and intracellular replication in vitro, and caused a significant virulence attenuation of both RH and Pru strains in mice. These results suggest that GRA76 is important for the growth of RH and Pru strains in vitro and in vivo.

Several GRAs are important for *T. gondii* growth, such as GRA17 that mediates nutrient uptake (Gold et al., 2015), and GRA44 and PPM3C which traffic important effectors (Blakely et al., 2020, Mayoral et al., 2020). MYR1 is essential for the export of proteins from the PV across the PVM into the host cell and host c-Myc upregulation (Franco et al., 2016). In a biochemical screen to identify MYR1-associating proteins, GRA76 together with PPM3C, GRA44, GRA45 and other proteins were identified by co-immunoprecipitation with MYR1 (Cygan et al., 2020). GRA44, GRA45 and MYR4 are essential for the translocation of GRA16 (Cygan et al., 2020, Wang et al., 2020c), and loss of PPM3C affects the export of GRA16 into the host cell. GRA16 and GRA24 are exported across the PVM and localize to the host nucleus (Bougdour et al., 2013, Braun et al., 2013). Although GRA76 was identified with MYR1 (Cygan et al., 2020), which plays an essential role in translocation of GRA proteins, deletion of *gra76* had no impact on the trafficking of GRA16 or GRA24 across the PVM into the host cell nucleus, indicating that GRA76 may not play a role in protein trafficking.

Some GRAs are important virulence factors of *T. gondii* (Hunter and Sibley, 2012),including GRA7 (Alaganan et al., 2014), GRA12 (Wang et al., 2020a), GRA45 (Wang et al., 2020c) and GRA60 (Nyonda et al., 2021). In this study, GRA76 was critical to the virulence of both type I RH and type II Pru strains. This result confirmed previous assumptions that GRA76 may represent a virulence factor

of *T. gondii* in mice (Young et al., 2019, Butterworth et al., 2022). However, the attenuated virulence level of RHΔ*gra76* was less pronounced than that of the PruΔ*gra76* strain. This might be attributed to the different virulence background of RH and Pru strains. The type I RH strain is highly virulent, and a single viable organism is lethal for laboratory mice (Sibley and Boothroyd, 1992, Su et al., 2002). Considering the significant in vitro growth defect of PruΔ*gra76* parasites, the marked attenuated virulence of PruΔ*gra76* may be due to its in vivo growth defect. The attenuated virulence of PruΔ*gra76* was restored in PruΔ*gra76*C when GRA76 was driven by its own promoter, but not in PruΔ*gra76*C_{Tub} when it was controlled by the tubulin promoter. This finding indicates that the stage-differential expression characteristic of GRA76 contributes to its activity and function regarding the restoration of virulence.

RNA-Seq analysis revealed that deletion of *gra76* in the Pru strain significantly upregulated expression of bradyzoite-associated genes such as BAG1 (Bohne et al., 1995), ENO1 (Kibe et al., 2005), CST1 (Tomita et al., 2013) and LDH2 (Yang and Parmley, 1997, Abdelbaset et al., 2017). A large number of tanscriptional factors play roles in bradyzoite differentiation, including *Toxoplasma* homologue of eukaryotic initiation factor 2 (TgIF2α), the plant-like Apetala-2 (AP2) transcriptional factors AP2XI-4, AP2IX-9, AP2IX-4, AP2IV-4 and AP2IV-3 (Jeffers et al., 2018). These transcriptional factors can activate or repress gene expression (Jeninga et al., 2019). In the present study, GRA76 was differently expressed in the tachyzoite and bradyzoite, and deletion of *gra76* increased the bradyzoite conversion rate. Thus, GRA76 expression may become down-regulated by a transcriptional regulatory factor when tachyzoites are subjected to stress to reduce parasite replication, and favour differentiation to the bradyzoite stage and formation of dormant cysts.

Live-attenuated vaccines are among the most effective vaccines, which can offer protection against *T. gondii* infection (Wang et al., 2017, Wang et al., 2019, Wang et al., 2020b, Liang et al., 2020). Based on the phenotype of the markedly attenuated virulence of PruΔ*gra76*, we evaluated the potential efficacy of PruΔ*gra76* as a live-attenuated vaccine against *T. gondii*. Immunization with PruΔ*gra76* partly protected mice from acute and chronic infection. However, PruΔ*gra76* did not provide 100% protection against challenge with the virulent parent RH strain. Therefore, PruΔ*gra76* is not effective as a live-attenuated vaccine strain, but could be used for generation of a double- or triple-attenuated knockout vaccine strain. High levels of total IgG, IgG1 and IgG2a antibodies were induced by immunization using PruΔ*gra76*. Thus, vaccination with PruΔ*gra76* can trigger Th1 and Th2 immune responses, with more dominance of the Th1 response, which is consistent with previous findings showing that protective immunity against *T. gondii* involves Th1-based immune responses (Hunter and Sibley, 2012, Yarovinsky, 2014).

In conclusion, this study demonstrates that GRA76, a newly characterized protein, is mainly localized in the PV of *T. gondii* and exhibits higher expression levels in tachyzoites than in bradyzoites. The deletion of *gra76* had a significant impact on *T. gondii* proliferation, causing a reduction in parasite virulence and brain cyst burden. Deletion of *gra76* in Pru strain resulted in up-regulation of genes

associated with bradyzoite differentiation and increased the Pru strain propensity for forming bradyzoites. Immunization with Pru*Δgra76* partly protected mice against acute and chronic infections. Our study adds more evidence to the growing importance of the role of GRAs in the replication, cyst formation and pathogenicity of *T. gondii*. Further work is needed to understand the exact role of GRA76 in parasite replication and bradyzoite formation, and to unravel the mechanisms that underpin GRA76 down-regulation in bradyzoites.

Acknowledgments

This work was supported by the Shanxi Provincial Key Research and Development Program, China (Grant No. 2022ZDYF126), the Natural Science Foundation of Gansu Province, China (Grant No. 23JRRA555), the National Natural Science Foundation of China (Grant No. 32002310), the National Key Research and Development Program of China (Grant Nos. 2021YFC2300800, 2021YFC2300802 and 2021YFC2300804), the Research Funding from Lanzhou Veterinary Research Institute, China (Grant No. CAASASTIP-JBGS-20210801), and Shanxi Provincial Agricultural and Rural Research Program, China (Grant No. LXXMsxnd202101)

Appendix A. . Supplementary Data

Supplementary data to this article can be found online at: xxx

References

A.E. Abdelbaset, B.A. Fox, M.H. Karram, M.R. Abd Ellah, D.J. Bzik, M.Igarashi. Lactate dehydrogenase in *Toxoplasma gondii* controls virulence, bradyzoite differentiation, and chronic infection. PLoS One., 12 (2017), p. e0173745

A. Alaganan, S.J. Fentress, K. Tang, Q. Wang, L.D. Sibley. *Toxoplasma* GRA7 effector increases turnover of immunity-related GTPases and contributes to acute virulence in the mouse. Proc Natl Acad Sci U S A., 111 (2014), pp. 1126-1131, 10.1073/pnas.1313501111

M.J. Bai, J.L. Wang, H.M. Elsheikha, Q.L. Liang, K. Chen, L.B. Nie, X.Q. Zhu. Functional characterization of dense granule proteins in *Toxoplasma gondii* RH strain using CRISPR-Cas9 system. Front Cell Infect Microbiol., 8 (2018), p. 300, 10.3389/fcimb.2018.00300

K. Barylyuk, L. Koreny, H. Ke, S. Butterworth, O.M. Crook, I. Lassadi, V. Gupta, E. Tromer, T. Mourier, T.J. Stevens, L.M. Breckels, A. Pain, K.S. Lilley, R.F. Waller. A comprehensive subcellular atlas of the *Toxoplasma* proteome via hyperLOPIT provides spatial context for protein functions. Cell Host Microbe., 28 (752–766) (2020), p. e759

W.J. Blakely, M.J. Holmes, G. Arrizabalaga. The secreted acid phosphatase domain-containing GRA44 from *Toxoplasma gondii* is required for c-Myc induction in infected cells., mSphere. 5 (2020), pp. e00877-00819, 10.1128/mSphere.00877-19

M. Blume, D. Rodriguez-Contreras, S. Landfear, T. Fleige, D. Soldati-Favre, R. Lucius, N. Gupta. Host-derived glucose and its transporter in the obligate intracellular pathogen *Toxoplasma gondii* are dispensable by glutaminolysis. Proc Natl Acad Sci U S A., 106 (2009), pp. 12998-13003, 10.1073/pnas.0903831106

W. Bohne, U. Gross, D.J. Ferguson, J. Heesemann. Cloning and characterization of a bradyzoite-specifically expressed gene (hsp30/bag1) of Toxoplasma gondii, related to genes encoding small heat-shock proteins of plants. Mol Microbiol., 16 (1995), pp. 1221-1230, 10.1111/j.1365-2958.1995.tb02344.x

A. Bougdour, E. Durandau, M. Brenier-Pinchart, P. Ortet, M. Barakat, S. Kieffer, A. Curt-Varesano, R. Curt-Bertini, O. Bastien, Y. Coute, H. Pelloux, M. Hakimi. Host cell subversion by *Toxoplasma* GRA16, an exported dense granule protein that targets the host cell nucleus and alters gene expression. Cell Host Microbe., 13 (2013), pp. 489-500, 10.1016/j.chom.2013.03.002

P.J. Bradley, C. Ward, S.J. Cheng, D.L. Alexander, S. Coller, G.H. Coombs, J.D. Dunn, D.J. Ferguson, S.J. Sanderson, J.M. Wastling, J.C. Boothroyd. Proteomic analysis of rhoptry organelles reveals many novel constituents for host-parasite interactions in *Toxoplasma gondii.* J Biol Chem., 280 (2005), pp. 34245-34258, 10.1074/jbc.M504158200

L. Braun, M. Brenier-Pinchart, M. Yogavel, A. Curt-Varesano, R. Curt-Bertini, T.Hussain, S. Kieffer-Jaquinod, Y. Coute, H. Pelloux, I. Tardieux, A. Sharma, H. Belrhali, A.Bougdour, M. Hakimi A Toxoplasma dense granule protein, GRA24, modulates the early immune response to infection by promoting a direct and sustained host p38 MAPK activation. J Exp Med., 210 (2013), pp. 2071-2086, 10.1084/jem.20130103

K.R. Buchholz, H.M. Fritz, X. Chen, B. Durbin-Johnson, D.M. Rocke, D.J. Ferguson, P.A. Conrad, J.C. Boothroyd. Identification of tissue cyst wall components by transcriptome analysis of in vivo and in vitro Toxoplasma gondii bradyzoites. Eukaryot Cell., 10 (2011), pp. 1637-1647, 10.1128/EC.05182-11

H.E. Bullen, H. Bisio, D. Soldati-Favre. The triumvirate of signaling molecules controlling Toxoplasma microneme exocytosis: Cyclic GMP, calcium, and phosphatidic acid. PLoS Pathog., 15 (2019), p. e1007670

S. Butterworth, F. Torelli, E.J. Lockyer, J. Wagener, O.R. Song, M. Broncel, M.R.G. Russell, A.C.A. Moreira-Souza, J.C. Young, M. Treeck. *Toxoplasma gondii* virulence factor ROP1 reduces parasite susceptibility to murine and human innate immune restriction. PLoS Pathog., 18 (2022), p. e1011021

B. Clough, E.M. Frickel. The Toxoplasma parasitophorous vacuole: an evolving host-parasite frontier Trends Parasitol., 33 (2017), pp. 473-488, 10.1016/j.pt.2017.02.007

A.M. Cygan, T.C. Theisen, A.G. Mendoza, N.D. Marino, M.W. Panas, J.C. Boothroyd. Coimmunoprecipitation with MYR1 identifies three additional proteins within the *Toxoplasma gondii* parasitophorous vacuole required for translocation of dense granule effectors into host cells., mSphere. 5 (2020), pp. e00858-00819, 10.1128/mSphere.00858-19

Elsheikha et al., 2021. H.M. Elsheikha, C.M. Marra, X.Q. Zhu. Epidemiology, pathophysiology, diagnosis, and management of cerebral toxoplasmosis. Clin Microbiol Rev., 34 (2021), pp. e00115-e00119, 10.1128/CMR.00115-19

M. Franco, M.W. Panas, N.D. Marino, M.C. Lee, K.R. Buchholz, F.D. Kelly, J.J. Bednarski, B.P. Sleckman, N. Pourmand, J.C. Boothroyd. A novel secreted protein, MYR1, is central to *Toxoplasma*'s manipulation of host cells., mBio. 7 (2016), pp. e02231-02215, 10.1128/mBio.02231-15

H.M. Fritz, K.R. Buchholz, X. Chen, B. Durbin-Johnson, D.M. Rocke, P.A. Conrad, J.C. Boothroyd Transcriptomic analysis of Toxoplasma development reveals many novel functions and structures specific to sporozoites and oocysts. PLoS One., 7 (2012), p. e29998.

D. Gold, A. Kaplan, A. Lis, G. Bett, E. Rosowski, K. Cirelli, A. Bougdour, S. Sidik, J. Beck, S. Lourido, P. Egea, P. Bradley, M. Hakimi, R. Rasmusson, J. Saeij. The *Toxoplasma* dense granule proteins GRA17 and GRA23 mediate the movement of small molecules between the host and the parasitophorous vacuole. Cell Host Microbe., 17 (2015), pp. 642-652, 10.1016/j.chom.2015.04.003

M.B. Griffith, C.S. Pearce, A.T. Heaslip. Dense granule biogenesis, secretion, and function in *Toxoplasma gondii.* J Eukaryot Microbiol., 69 (2022), p. e12904

R. Guevara, B. Fox, A. Falla, D. Bzik. *Toxoplasma gondii* intravacuolar-network-associated dense granule proteins regulate maturation of the cyst matrix and cyst wall., mSphere. 4 (2019), pp. e00487-00419, 10.1128/mSphere.00487-19

R. Guevara, B. Fox, D. Bzik. *Toxoplasma gondii* parasitophorous vacuole membrane-associated dense granule proteins regulate maturation of the cyst wall., mSphere. 5 (2020), pp. e00851-00819, 10.1128/mSphere.00851-19

R.B. Guevara, B.A. Fox, D.J. Bzik. A family of *Toxoplasma gondii* genes related to GRA12 regulate cyst burdens and cyst reactivation., mSphere. 6 (2021), pp. e00182-00121, 10.1128/mSphere.00182-21.

M.A. Hakimi, P. Olias, L.D. Sibley. *Toxoplasma* effectors targeting host signaling and transcription. Clin Microbiol Rev., 30 (2017), pp. 615-645, 10.1128/CMR.00005-17

D.P. Hong, J.B. Radke, M.W. White. Opposing transcriptional mechanisms regulate Toxoplasma development. mSphere., 2 (1) (2017), pp. e00347-00316, 10.1128/mSphere.00347-16

C.A. Hunter, L.D. Sibley. Modulation of innate immunity by Toxoplasma gondii virulence effectors Nat Rev Microbiol., 10 (2012), pp. 766-778, 10.1038/nrmicro2858.

V. Jeffers, Z. Tampaki, K. Kim, W.J. Sullivan Jr.A latent ability to persist: differentiation in *Toxoplasma gondii.* Cell Mol Life Sci., 75 (2018), pp. 2355-2373, 10.1007/s00018-018-2808-x

M.D. Jeninga, J.E. Quinn, M. Petter. ApiAP2 transcription factors in apicomplexan parasites Pathogens., 8 (2) (2019), p. 47, 10.3390/pathogens8020047

M.K. Kibe, A. Coppin, N. Dendouga, G. Oria, E. Meurice, M. Mortuaire, E. Madec, S. Tomavo Transcriptional regulation of two stage-specifically expressed genes in the protozoan parasite Toxoplasma gondii. Nucleic Acids Res., 33 (2005), pp. 1722-1736, 10.1093/nar/gki314.

D. Kim, B. Langmead, S.L. Salzberg. HISAT: a fast spliced aligner with low memory requirements Nat Methods., 12 (2015), pp. 357-360, 10.1038/nmeth.3317.

S. Krishnamurthy, P. Maru, Y. Wang, M.A. Bitew, D. Mukhopadhyay, Y. Yamaryo-Botte, T.C. Paredes-Santos, L.O. Sangare, C. Swale, C.Y. Botte, J.P.J. Saeij. CRISPR screens identify Toxoplasma genes that determine parasite fitness in interferon gamma-stimulated human cells., mBio. 14 (2023), p. e0006023.

B. Li, C.N. Dewey. RSEM: accurate transcript quantification from RNA-Seq data with or without a reference genome. BMC Bioinformatics., 12 (2011), p. 323, 10.1186/1471-2105-12-323

R. Li, Y. Li, K. Kristiansen, J. Wang. SOAP: short oligonucleotide alignment program. Bioinformatics., 24 (2008), pp. 713-714, 10.1093/bioinformatics/btn025.

S. Li, J. Liu, H. Zhang, Z. Sun, Z. Ying, Y. Wu, J. Xu, Q. Liu. Toxoplasma gondii glutathione S-transferase 2 plays an important role in partial secretory protein transport. FASEB J., 35 (2021), p. e21352.

Q.L. Liang, L.X. Sun, H.M. Elsheikha, X.Z. Cao, L.B. Nie, T.T. Li, T.S. Li, X.Q. Zhu, J.L.Wang. RHΔgra17Δnpt1 strain of Toxoplasma gondii elicits protective immunity against acute, chronic and congenital Toxoplasmosis in mice. Microorganisms., 8 (2020), p. 352, 10.3390/microorganisms8030352

Q.L. Liang, L.B. Nie, T.T. Li, H.M. Elsheikha, L.X. Sun, Z.W. Zhang, D.Y. Zhao, X.Q. Zhu, J.L. Wang. Functional characterization of 17 protein serine/threonine phosphatases in Toxoplasma gondii using CRISPR-Cas9 system. Front Cell Dev Biol., 9 (2021), Article 738794, 10.3389/fcell.2021.738794.

M.I. Love, W. Huber, S. Anders. Moderated estimation of fold change and dispersion for RNA-seq data with DESeq2. Genome Biol., 15 (2014), p. 550, 10.1186/s13059-014-0550-8.

B.J. Luft, J.S. Remington. Toxoplasmic encephalitis in AIDS. Clin Infect Dis., 15 (1992), pp. 211-222, 10.1093/clinids/15.2.211

J. Mayoral, T. Tomita, V. Tu, J.T. Aguilan, S. Sidoli, L.M. Weiss. Toxoplasma gondii PPM3C, a secreted protein phosphatase, affects parasitophorous vacuole effector export. PLoS Pathog., 16 (2020), p. e1008771.

J. Mayoral, R.B. Guevara, Y. Rivera-Cuevas, V. Tu, T. Tomita, J.D. Romano, L. Gunther-Cummins, S. Sidoli, I. Coppens, V.B. Carruthers, L.M. Weiss. Dense granule protein GRA64 interacts with host cell ESCRT proteins during Toxoplasma gondii infection., mBio. 13 (2022), p. e0144222.

S.M. Nadipuram, A.C. Thind, S. Rayatpisheh, J.A. Wohlschlegel, P.J. Bradley. Proximity biotinylation reveals novel secreted dense granule proteins of *Toxoplasma gondii* bradyzoites. PLoS One., 15 (2020), p. e0232552

M. Nyonda, P. Hammoudi, S. Ye, J. Maire, J. Marq, M. Yamamoto, D. Soldati-Favre. *Toxoplasma gondii* GRA60 is an effector protein that modulates host cell autonomous immunity and contributes to virulence. Cell Microbiol., 23 (2021), p. e13278

K.J. Pittman, M.T. Aliota, L.J. Knoll. Dual transcriptional profiling of mice and *Toxoplasma gondii* during acute and chronic infection. BMC Genomics., 15 (2014), p. 806, 10.1186/1471-2164-15-806

J.B. Radke, O. Lucas, E.K. De Silva, Y. Ma, W.J. Sullivan Jr., L.M. Weiss, M. Llinas, M.W. White. ApiAP2 transcription factor restricts development of the *Toxoplasma*tissue cyst. Proc Natl Acad Sci U S A., 110 (2013), pp. 6871-6876, 10.1073/pnas.1300059110

Y. Rivera-Cuevas, J. Mayoral, M. Di Cristina, A.E. Lawrence, E.B.Olafsson, R.K. Patel, D. Thornhill, B.S. Waldman, A. Ono, J.Z. Sexton, S. Lourido, L.M. Weiss, V.B. Carruthers. Toxoplasma gondii exploits the host ESCRT machinery for parasite uptake of host cytosolic proteins. PLoS Pathog., 17 (2021), p. e1010138.

F. Robert-Gangneux, M.L. Darde. Epidemiology of and diagnostic strategies for toxoplasmosis Clin Microbiol Rev., 25 (2012), pp. 264-296, 10.1128/CMR.05013-11

A. Rosenberg, L.D. Sibley. *Toxoplasma gondii* secreted effectors co-opt host repressor complexes to inhibit necroptosis. Cell Host Microbe., 29 (1186–1198) (2021), p. e1188

L.D. Sibley, J.C. Boothroyd. Virulent strains of *Toxoplasma gondii* comprise a single clonal lineage. Nature., 359 (1992), pp. 82-85, 10.1038/359082a0

C. Su, D.K. Howe, J.P. Dubey, J.W. Ajioka, L.D. Sibley. Identification of quantitative trait loci controlling acute virulence in *Toxoplasma gondii.* Proc Natl Acad Sci U S A., 99 (2002), pp. 10753-10758, 10.1073/pnas.172117099

T. Tomita, D.J. Bzik, Y.F. Ma, B.A. Fox, L.M. Markillie, R.C. Taylor, K. Kim, L.M. Weiss. The *Toxoplasma gondii* cyst wall protein CST1 is critical for cyst wall integrity and promotes bradyzoite persistence. PLoS Pathog., 9 (2013), p. e1003823

V. Tu, J. Mayoral, T. Sugi, T. Tomita, B. Han, Y.F. Ma, L.M. Weiss. Enrichment and proteomic characterization of the cyst wall from *in vitro Toxoplasma gondii* cysts., mBio. 10 (2019), pp. e00469-00419, 10.1128/mBio.00469-19

V. Tu, J. Mayoral, R.R. Yakubu, T. Tomita, T. Sugi, B. Han, T. Williams, Y. Ma, L.M. Weiss. MAG2, a *Toxoplasma gondii* bradyzoite stage-specific cyst matrix protein mSphere., 5 (1) (2020), pp. e00100-e00120, 10.1128/mSphere.00100-20

V. Tu, T. Tomita, T. Sugi, J. Mayoral, B. Han, R.R. Yakubu, T. Williams, A. Horta, Y. Ma, L.M. Weiss. The *Toxoplasma gondii* cyst wall interactome., mBio. 11 (2020), pp. e02699-02619, 10.1128/mBio.02699-19

J.L. Wang, H.M. Elsheikha, W.N. Zhu, K. Chen, T.T. Li, D.M. Yue, X.X. Zhang, S.Y. Huang, X.Q. Zhu. Immunization with *Toxoplasma gondii* GRA17 deletion mutant induces partial protection and survival in challenged mice. Front Immunol., 8 (2017), p. 730, 10.3389/fimmu.2017.00730

J.L. Wang, N.Z. Zhang, T.T. Li, J.J. He, H.M. Elsheikha, X.Q. Zhu. Advances in the development of anti-*Toxoplasma gondii* vaccines: challenges, opportunities, and perspectives. Trends Parasitol., 35 (2019), pp. 239-253, 10.1016/j.pt.2019.01.005

J.L. Wang, M.J. Bai, H.M. Elsheikha, Q.L. Liang, T.T. Li, X.Z. Cao, X.Q. Zhu. Novel roles of dense granule protein 12 (GRA12) in *Toxoplasma gondii* infection. Faseb J., 34 (2020), pp. 3165-3178, 10.1096/fj.201901416RR

J.L. Wang, Q.L. Liang, T.T. Li, J.J. He, M.J. Bai, X.Z. Cao, H.M. Elsheikha, X.Q. Zhu. *Toxoplasma gondii* tkl1 deletion mutant is a promising vaccine against acute, chronic, and congenital toxoplasmosis in mice. J Immunol., 204 (2020), pp. 1562-1570, 10.4049/jimmunol.1900410

J.L. Wang, T.T. Li, H.M. Elsheikha, Q.L. Liang, Z.W. Zhang, M. Wang, L.D. Sibley, X.Q. Zhu. The protein phosphatase 2A holoenzyme is a key regulator of starch metabolism and bradyzoite differentiation in *Toxoplasma gondii.* Nat Commun., 13 (2022), p. 7560, 10.1038/s41467-022-35267-5

Y. Wang, L. Sangare, T. Paredes-Santos, M. Hassan, S. Krishnamurthy, A.Furuta, B. Markus, S. Lourido, J. Saeij. Genome-wide screens identify Toxoplasma gondii determinants of parasite fitness in IFNγ-activated murine macrophages. Nat Commun., 11 (2020), p. 5258, 10.1038/s41467-020-18991-8

Y. Wang, L.O. Sangare, T.C. Paredes-Santos, J.P.J. Saeij. *Toxoplasma* mechanisms for delivery of proteins and uptake of nutrients across the host-pathogen interface. Annu Rev Microbiol., 74 (2020), pp. 567-586, 10.1146/annurev-micro-011720-122318

Z.D. Wang, W.S., Liu HH, Ma HY, Li ZY, Wei F, Zhu XQ, Liu Q., Prevalence and burden of *Toxoplasma gondii* infection in HIV-infected people: a systematic review and meta-analysis Lancet HIV., 4 (2017), pp. e177-e188, 10.1016/S2352-3018(17)30005-X

S. Yang, S.F. Parmley. *Toxoplasma gondii* expresses two distinct lactate dehydrogenase homologous genes during its life cycle in intermediate hosts. Gene., 184 (1997), pp. 1-12, 10.1016/s0378-1119(96)00566-5

F. Yarovinsky. Innate immunity to *Toxoplasma gondii* infection. Nat Rev Immunol., 14 (2014), pp. 109-121, 10.1038/nri3598

J. Young, C. Dominicus, J. Wagener, S. Butterworth, X. Ye, G. Kelly, M. Ordan, B. Saunders, R. Instrell, M. Howell, A. Stewart, M. Treeck. A CRISPR platform for targeted *in vivo* screens identifies *Toxoplasma gondii* virulence factors in mice. Nat Commun., 10 (2019), p. 3963, 10.1038/s41467-019-11855-w

X.N. Zheng, J.L. Wang, H.M. Elsheikha, M. Wang, Z.W. Zhang, L.X. Sun, X.C. Wang, X.Q. Zhu, T.T. Li. Functional characterization of 15 novel dense granule proteins in *Toxoplasma gondii* using the CRISPR-Cas9 system. Microbiol Spectr., 11 (2023), p. e0307822

W.B. Zheng, Y. Zou, J.J. He, H.M. Elsheikha, G.H. Liu, M.H. Hu, S.L. Wang, X.Q.Zh.Glo bal profiling of lncRNAs-miRNAs-mRNAs reveals differential expression of coding genes and non-coding RNAs in the lung of beagle dogs at different stages of *Toxocara canis* infection. Int J Parasitol., 51 (2021), pp. 49-61, 10.1016/j.ijpara.2020.07.014